CHEMISTRY OF MATERIALS

ARTICLE

pubs.acs.org/cm

Assembly and Characterization of Well-Defined High-Molecular-Weight Poly(*p*-phenylene) Polymer Brushes

Jose Alonzo,[*,†] Jihua Chen,[‡] Jamie Messman,[‡] Xiang Yu,[§] Kunlun Hong,[‡] Suxiang Deng,[⊥] Onome Swader,[⊥] Mark Dadmun,[§,⊥] John F. Ankner,[†] Phillip Britt,[§] Jimmy W. Mays,[‡,§,⊥] Massimo Malagoli,[#,∥] Bobby G. Sumpter,[‡,∥] Jean-Luc Brédas,[#] and S. Michael Kilbey, II[*,‡,⊥]

[†]Neutron Scattering Science Division, [‡]Center for Nanophase Materials Sciences, [§]Chemical Sciences Division, and [∥]Computer Science and Mathematics Division, Oak Ridge National Laboratory, Oak Ridge, Tennessee 37831, United States

[⊥]Department of Chemistry, University of Tennessee, Knoxville, Tennessee 37996, United States

[#]School of Chemistry and Biochemistry, Center for Computational Molecular Science and Technology, and Center for Organic Photonics and Electronics, Georgia Institute of Technology, Atlanta, Georgia 30332-0400, United States

Supporting Information

ABSTRACT: The assembly and characterization of well-defined, end-tethered poly(*p*-phenylene) (PPP) brushes having high molecular weight, low polydispersity and high 1,4-stereoregularity are presented. The PPP brushes are formed using a precursor route that relies on either self-assembly or spin coating of high molecular weight (degrees of polymerizations 54, 146, and 238) end-functionalized poly(1,3-cyclohexadiene) (PCHD) chains from benzene solutions onto silicon or quartz substrates, followed by aromatization of the end-attached PCHD chains on the surface. The approach allows the thickness (grafting density) of the brushes to be easily varied. The dry brushes before and after aromatization are characterized by ellipsometry, atomic force microscopy, grazing angle attenuated total reflectance Fourier transform infrared spectroscopy, and UV-Vis spectroscopy. The properties of the PPP brushes are compared with those of films made using oligoparaphenylenes and with ab initio density functional theory simulations of optical properties. Our results suggest conversion to fully aromatized, end-tethered PPP polymer brushes having effective conjugation lengths of 5 phenyl units.

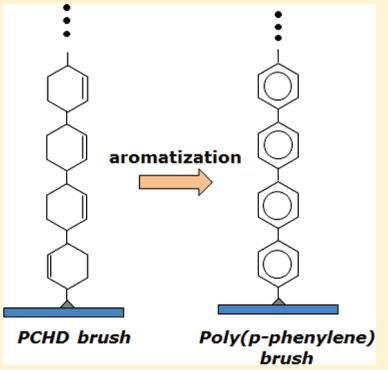

KEYWORDS: poly(*para*-phenylene), polymer brush, thin film, electronic structure

INTRODUCTION

Conjugated polymers are the basis for many future developments in areas such as energy conversion, energy storage, biosensors, and many devices that take advantage of their electrical, magnetic, and optical properties.[1−3] They are used as active layers in organic optoelectronic devices or organic integrated circuits. Although there has been considerable progress in these areas of research, many of the fundamental aspects that govern the performance of these devices are still largely unexplored or unresolved. Among these fundamental aspects, control of morphology at the nanoscale has been recognized as one of paramount importance.[4−6] As many devices rely on tight control of interfaces, research focused on elucidating the links between nanoscale design, assembly, structure and properties is crucially important. Along these lines, conjugated polymers confined to interfaces in a "brushlike" configuration represent an important model system. Not only do these systems allow structure−property relationships of well-defined systems to be studied, but the organized structure of a brush layer offers the possibility of improved or enhanced optoelectronic properties when π-conjugated materials are used. For example, it has been shown by Niko et al. that the optical absorbance of oriented films of para-hexaphenyl, the six unit oligomer of poly(para-phenylene) (PPP), exhibits strong anisotropy effects.[7]

PPP is regarded as one of the most promising polymers for optoelectronic applications[8] due to its high thermal and chemical stability[9] and high conductivity when doped.[10] Unfortunately, solubility issues inherent in high-molecular-weight unsubstituted PPPs (and other conjugated polymers) create processing and characterization problems that have hindered detailed studies of structure−property relationships of these macromolecular materials. To address this problem, low molecular weight PPPs or oligomeric paraphenylenes (OPPs) have been studied extensively, both in solution and as thin films, and the properties of high molecular weight PPPs have been extrapolated from these results.[11−13] Thus, not only is it challenging to create devicelike constructs based on high-molecular-weight PPPs, but the synthetic approaches typically used to create high molecular weight PPPs often preclude rigorous characterization of molecular parameters such as molecular weight, polydispersity, and chain

Received: June 26, 2011
Revised: August 24, 2011
Published: September 19, 2011

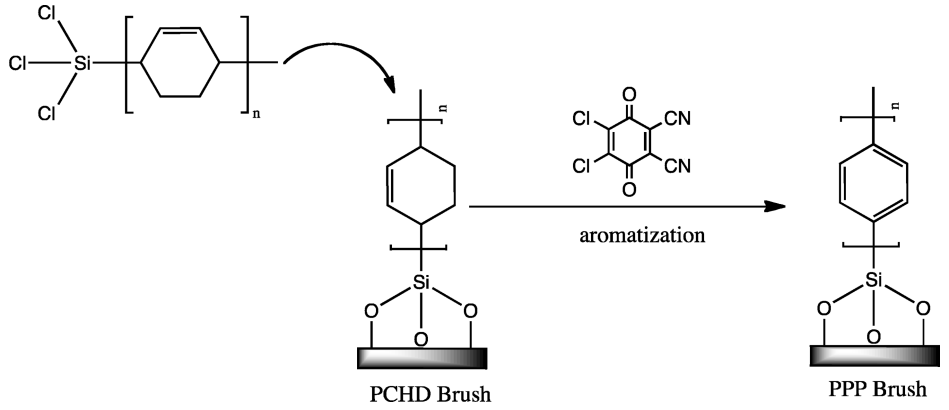

Figure 1. Approach used to obtain well-defined PPP brushes based on in situ aromatization of surface-tethered PCHD precursor chains.

Table 1. Molecular Characteristics of the PCHD Precursor Polymers

polymer	M_n (kg/mol)	DP	PDI	1,4-/1,2-CHD units (mol %)
4K PCHD	4.3	54	1.09	95
11K PCHD	11.7	146	1.07	93
19K PCHD	19.0	239	1.07	93

microstructure. As a result, the ability to relate optoelectronic properties and device performance to fundamental characteristics of the chainlike nature of PPP remains elusive.[13−18]

To address this limitation, we describe the preparation of well-defined PPP brushes using a polymer precursor route, whereby end-functionalized poly(1,3-cyclohexadiene) (PCHD) chains are chemically grafted by one end to a solid substrate and aromatized in situ, as shown in Figure 1. This approach provides access to high molecular weight materials having low polydispersity, and the use of polar additives can be effectively used to tune chain microstructure by altering the ratio of 1,4 versus 1,2 addition.[30−33] Polymer brushes—layers of end-anchored chains arrayed at solid-fluid interfaces—have served as archetypes for examining structure−property relationships of flexible polymer chains for over two decades.[19−28] As there are, to the best of our knowledge, no studies of the properties of well-defined confined PPP chains (PPP brushes), in addition to describing the formation and characterization of well-defined high-molecular-weight PPP brushes, we make comparisons with the optical absorption properties of spin-coated thin films of OPPs as well as with density functional theory (DFT) calculations.

EXPERIMENTAL SECTION

Materials Preparation. Three well-defined poly(1,3-cyclohexadiene) (PCHD) polymers having a trichlorosilane end-group were synthesized by high vacuum anionic polymerization techniques using custom-made all-glass reactors with break-seals.[29,30] As described by Hong and Mays[30] and Natori et al.,[31−33] polar additives are used in anionic polymerizations to control the chain microstructure. Here, 1,4-diazabicycly[2.2.2]octane (DABCO) is used to create PCHDs having high 1,4 content, and the molar ratio of 1,4- versus 1,2-addition was characterized using ^{1}H NMR.[30] The molecular characteristics of the PCHD polymers are shown in Table 1. The PCHD polymers were characterized before adding trichlorosilane to end-cap the polymer. A series of oligomers identified as OPP-2 to OPP-7 (where the number denotes the number of phenyl rings), generously provided by R. Rathore, were also studied for comparison. Details of the synthesis and optoelectronic solution properties of these OPPs have been reported previously.[11]

Brush Formation. All solution preparations required for brush formation were performed inside a glovebox under controlled conditions (H_2O and O_2 < 0.1 ppm). Rigorously dried solvents were used to prevent reaction (hydrolysis) of the trichlorosilane functional group and oxidation of the PCHD. PCHD brushes were formed by self-assembly and by spin coating from dilute solutions in benzene (Fisher, 99%) onto silicon and quartz substrates. Benzene was purified by distillation on a high vacuum line following standard procedures.[29] After spin coating (2500 rpm, 15 s), the samples were annealed under a vacuum at 160 °C for 24 h and then sonicated in benzene for 1 h to remove any nongrafted polymer chains. In the case of the brushes made by spin coating, the layer thicknesses (and thus the grafting densities) could be varied rather widely by changing the concentration of PCHD in solution.

After formation and characterization of the PCHD brushes, they were aromatized in situ using 2,3-dichloro-5,6-dicyanobenzoquinone, (DDQ, Aldrich, 98%) to produce PPP brushes. The basic protocol for the aromatization reaction was adapted from the conditions used to aromatize PCHD in solution.[31−33] In short, 350 mL of 1,2-dichlorobenzene (DCBz, Aldrich, 99%) is introduced into a four-necked reactor vessel containing the substrates. The solution is then agitated using a magnetic bar and dry N_2 is bubbled through the system for 30 min. The flask is immersed in an oil bath and the temperature increased to 120 °C, at which point 0.5 g of DDQ is added. The flask with the surfaces is maintained, with agitation, at 120 °C and under a N_2 atmosphere for 36 h, after which time the surfaces are removed and rinsed sequentially with acetone, toluene, and benzene, and then sonicated in benzene for 1 h. After this final step, the surfaces are dried with N_2 stream and stored in an argon-filled glovebox until characterized.

Characterization Methods. The dry brushes before and after aromatization were characterized by ellipsometry, atomic force microscopy (AFM), grazing angle attenuated total reflectance Fourier transform infrared spectroscopy (GATR-FTIR), and UV-Vis spectroscopy. Thin films of the OPP oligomers were made by spin coating (2500 rpm, 15 s) from benzene solutions (nominal concentration 0.5 wt %) onto quartz surfaces and characterized using UV-Vis spectroscopy.

Fourier-Transform Infrared Spectroscopy (FTIR). FTIR was performed on a Vertex 70 FTIR spectrometer from Bruker Optics using either a deuterated triglycine sulfate (DTGS) or a liquid nitrogen cooled mercury−cadmium-telluride (MCT) detector. For transmission mode experiments, background spectra were obtained from a bare quartz substrate, while for attenuated total reflectance (ATR) measurements the background spectra were acquired using the clean ATR crystal. The ATR FTIR spectra for bulk PCHD samples (powders) and brushes (thin

dx.doi.org/10.1021/cm201819p |*Chem. Mater.* 2011, 23, 4367–4374

films) were collected using a MVP Star accessory with a diamond IRE crystal, and a GATR accessory from Harrick Scientific with a germanium crystal, respectively.

Ellipsometry. A J.A. Woollam M-2000U variable angle spectroscopic ellipsometer with an X-Y mapping stage was used to measure ellipsometric thickness of the thin films. Estimates of the thickness of PCHD and PPP brushes were obtained by fitting the ellipsometric angles, Ψ and Δ, over the entire wavelength range, 200 nm < λ < 990 nm, representing the brushes as slabs of uniform optical density described by a Cauchy model atop silicon substrates (represented as a bulk silicon slab with a silicon oxide film of nominally 15 Å thickness). Multiple measurements were made on each sample, and thicknesses reported are the average of at least three different measurements.

Ultraviolet-Visible (UV-Vis) Spectroscopy. A Varian Cary 5000 was used to measure optical absorbance over the wavelength range 200 < λ < 800 nm. In each case a background spectrum was collected using a clean, blank quartz substrate.

Atomic Force Microscopy (AFM). The surface topography of PCHD and PPP brushes was imaged using a Dimension 3100 scanning probe microscope from Veeco Instruments. Height and phase images were collected simultaneously in tapping mode using SiN tips. Roughness analysis of the images was performed using the instrument software.

Computational Method. Density Functional Theory (DFT) calculations were used to study the structure and optical absorption for the OPPs. Both isolated chains and oligomers end-attached to a silica cluster simulating the quartz surface were studied. Calculations were performed using the B3LYP hybrid functional.[34,35] Electronic absorptions were determined at the time-dependent (TD) DFT level,[36−38] using the Tamm−Dancoff approximation.[39] We performed full geometry optimization followed by TD-DFT calculations using the NWChem program.[40] For these calculations we used the effective core potential LANL2DZ basis set.[41−43] In order to validate the LANL2DZ results, all-electron calculations with the larger 6-311G(d,p) basis[44] for the isolated oligomers only, were performed. The larger basis predicts transition energies that are blue-shifted by 0.02−0.12 eV (see the Supporting Information for details). On the basis of recent benchmark studies assessing the accuracy of various DFT functionals for TD-DFT calculations of excited states of organic molecules,[45,46] we expect the computed energies to be accurate within 0.25−0.30 eV.

Simulation of the Quartz Surface. The basic building block of silica is a tetrahedron with a silicon atom at the center and four oxygen atoms at the corners. These tetrahedra are connected in a network, with each oxygen bridging two silicon atoms. For our simulation we used a cluster of three tetrahedra connected to a central silicon atom, acting as attachment point for the OPP chain. All dangling bonds were saturated by hydrogen, resulting in the cluster $Si_4O_{12}H_{10}$ (a sketch of the structure is given in the Supporting Information). After geometry optimization at the B3LYP/LANL2DZ level, this cluster exhibits a HOMO−LUMO gap of 8.3 eV, which is reasonably close to the experimental band gap of amorphous silica, measured at 8.9 eV.[47]

RESULTS AND DISCUSSION

In this work, we examined both spin-coating and self-assembly from dilute solution as a means of making PCHD brushes. Because approaches using self-assembly gave layers of small thickness (~2.5 nm) and low tethering densities, spin coating was used to create more dense layers of controllable thickness. Figure 2 shows the range of thicknesses and grafting densities achieved for PCHD brushes formed by spin coating from benzene solutions onto silicon substrates. The layer thickness, t, is related to the tethering density, σ, by $\sigma = t\rho N_{Av}/M_n$, where ρ is the bulk density of the polymer, N_{Av} is Avogadro's number, and M_n is the number-average molecular weight of the polymer.

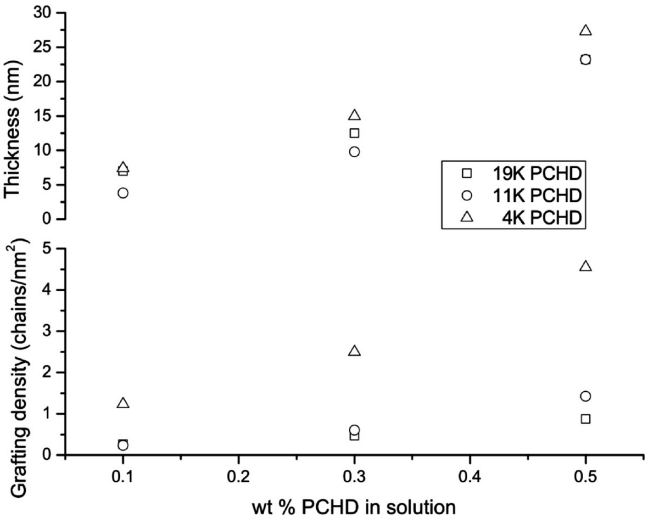

Figure 2. Dry layer thicknesses and grafting densities obtained from spin coated PCHD brushes. To control the thickness (grafting density) of the spin-coated brushes, we varied the concentration of the spin-coating solution (0.5, 0.3, and 0.1 wt %).

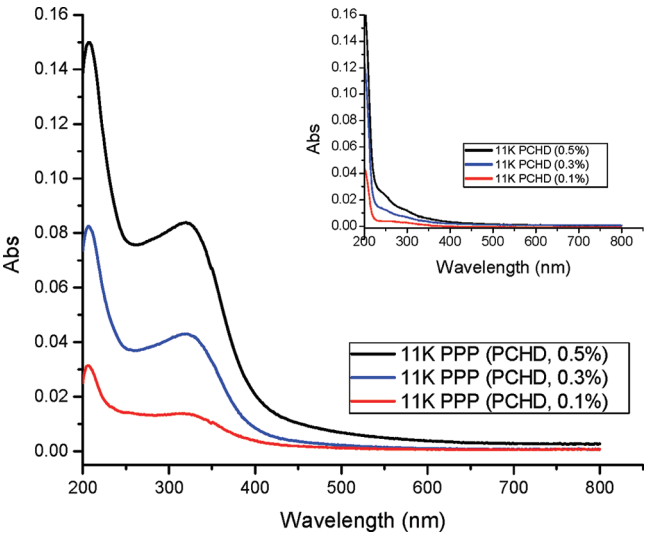

Figure 3. UV-Vis spectra of PPP brushes made by aromatization of the precursor PCHD brushes created by spin coating PCHDs at concentrations indicated in the legend. As a result of the aromatization reaction, the PPP brush shows two new absorption bands centered at 209 and ~320 nm. The inset graph shows the UV-Vis absorption spectra of the precursor PCHD brushes with the number in brackets indicating the solution concentration from which the brushes were spin-coated.

The specific values for the grafting densities for the three polymers and at the three solution concentrations can be found in the Supporting Information. The grafting density of PCHD brushes can be controlled from low density (~0.2 chains/nm^2) to high density (>4.5 chains/nm^2). In agreement with expectations and results described in the literature for end-attached polymer brushes made by trichlorosilane end-functionalized polystyrene chains on silicon wafers,[48] larger thicknesses are obtained when smaller molecular weights are used, and higher concentrations lead to more dense films of greater thickness.

dx.doi.org/10.1021/cm201819p |*Chem. Mater.* 2011, 23, 4367–4374

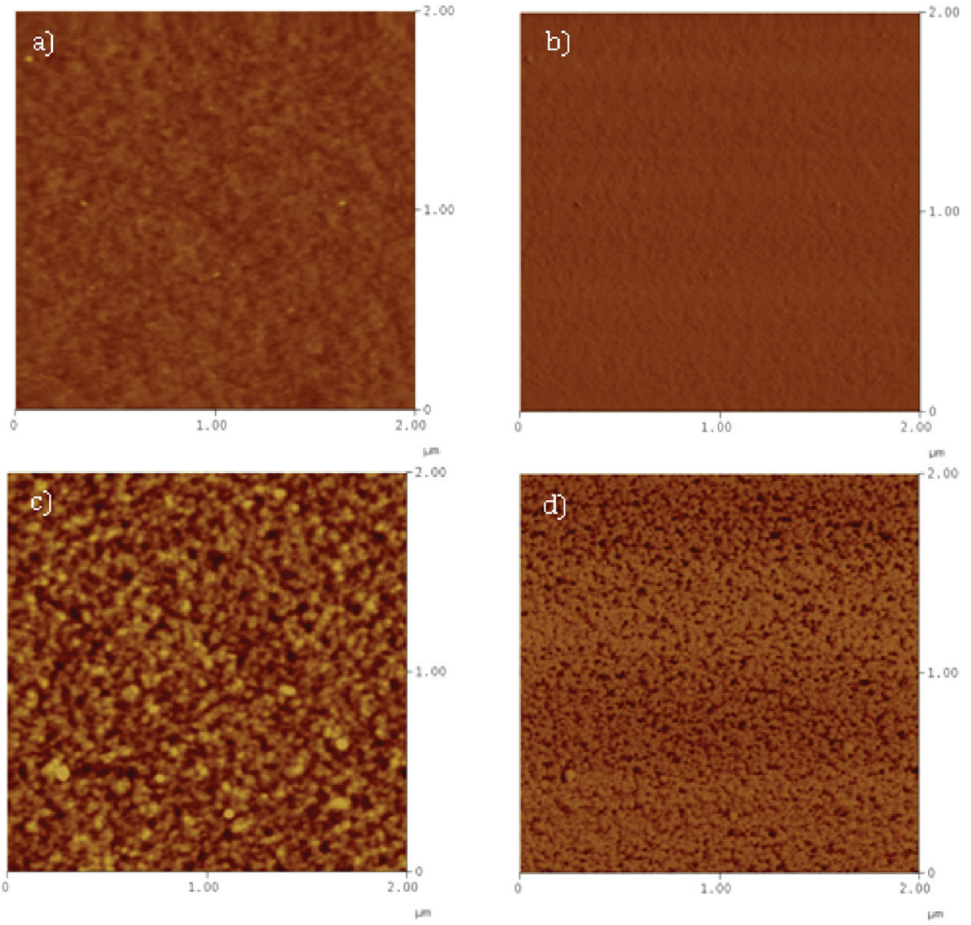

Figure 4. Typical AFM images obtained for dry PCHD and PPP brushes; (a) Height image for PCHD brush, (b) phase image for PCHD brush, c) height image for PPP brush, (d) phase image for PPP brush. The *z*-range scale for the height images obtained by AFM is 10 nm, and the phase scale is 30 and 20° for PCHD and PPP, respectively. The surfaces remain uniformly covered even after the aromatization process.

To confirm that the end-tethered PCHD chains exist in the brush regime, we compare one-half the distance between grafting points, d, to the radius-of-gyration, R_g, of the corresponding PCHD chain. The former is calculated from the measured grafting density assuming that each chain occupies a circular area on the surface,[26] and the latter is estimated using the Benoit−Doty expression for a worm-like chain, parametrized based on previous measurements of PCHD chain size.[49] The resultant values of $d/2R_g$ are less than unity, ranging from 0.13 to 0.34 (see Table S1 in the Supporting Information), indicating that the PCHD chains are crowded on the surface because of tethering, and thus adopt extended conformations characteristic of polymer brushes.

To examine optical properties of the brushes, in parallel we performed depositions onto quartz substrates in parallel using the same stock solutions and spin-coating conditions; thus it is expected and assumed that the dry layer thicknesses (tethering densities) of the brushes assembled on quartz substrates are approximately the same as those formed on silicon wafers. UV-Vis absorption spectra for PCHD brushes on quartz substrates assembled from three different solution concentrations for the 11K PCHD are presented in the inset graph of Figure 3. (Similar results were obtained for 4K and 19K PCHDs, and these data are presented in the Supporting Information).

As can be seen in Figure 3, the intensity of the measured optical absorbance changes with the concentration of PCHD in the solution used for spin coating − those brushes created from more concentrated solutions give rise to larger absorbance (for a given wavelength), reflecting the increase in thicknesses (and grafting densities) of the brushes. Each PCHD or PPP brush of a given molecular weight displayed a linear relationship between the measured UV absorption (at fixed wavelength) and the thickness measured by ellipsometry (on silicon substrates). Figure S1 in the Supporting Information shows the correlation used to estimate the thicknesses of PCHD brushes on quartz substrates.

Images a and b in Figure 4 show AFM results typical of the PCHD brushes formed by spin coating on silicon substrates. As can be seen from the images, PCHD brushes formed by spin coating are smooth and homogeneous, having surface roughness in the range of 0.45−0.8 nm. Also shown in Figure 4 are surface topography images for one of the aromatized PCHD brushes. Several regions on a variety of samples were imaged, and all showed full coverage of the surface, suggesting no apparent scouring of grafted chains from the surfaces after the aromatization reaction. This finding along with results from FTIR (discussed below) and UV-Vis spectroscopy studies confirm that the reaction conditions used are suitable for the ultrathin films. A variety of attempts were made to aromatize the PCHD brushes in situ. As described in the Experimental section, we found that the quinone DDQ at 120 °C was suitable for the

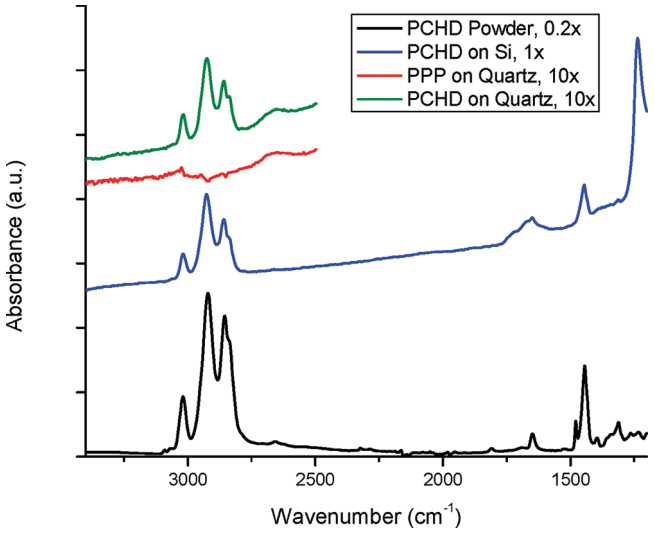

Figure 5. FTIR spectra of PCHD and PPP brushes on silicon and on quartz. The samples on silicon were obtained using grazing incidence ATR and those on quartz were acquired in transmission mode. A spectrum of PCHD powder measured using ATR is provided for comparison. All PCHD samples show stretching modes characteristic of methylene groups, which disappear after the dehydrogenation reaction (PPP brush). Because quartz absorbs below 2300 cm^{-1}, only a portion of the spectrum is shown. To facilitate comparisons, the spectra of the powder and of the brushes on quartz are scaled as indicated in the legend.

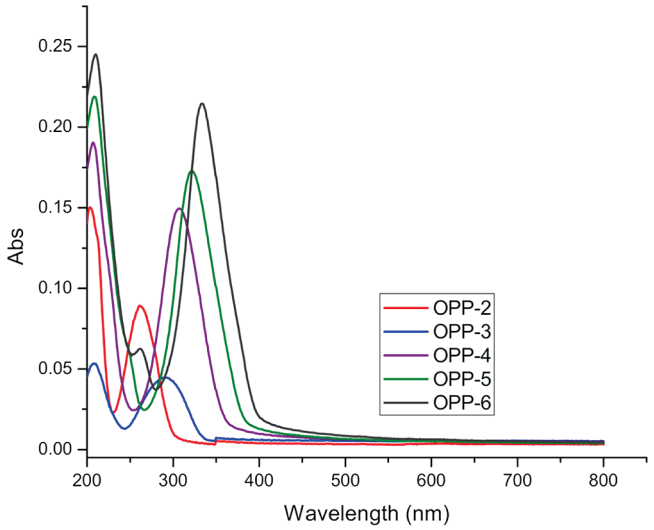

Figure 6. UV-Vis spectra of OPP thin films created by spin-coating. The position of the second peak changes with increasing conjugation length.

aromatization reaction. Temperatures significantly above 120 °C were found to scour chains from the surface, and temperatures below 120 °C led to incomplete aromatization, as observed through UV-Vis spectroscopy. As can be seen in Figure 4, there is a clear difference between the smooth PCHD brushes and the aromatized (PPP) ones: the rms roughness has increased to ~2 nm, which we assume is due to aggregation of the PPP chains.

Figure 5 shows various FTIR spectra acquired from PCHD and PPP brushes. The GATR-FTIR spectrum obtained for a representative PCHD brush on a silicon surface shows the characteristic absorption bands due to $-CH_2-$ stretching modes (bands between 3018 and 2858 cm^{-1}),[33] and these bands are also observed in the spectrum acquired using PCHD powder. Figure 5 also shows spectra measured for an aromatized 11K PPP brush and the corresponding 11K precursor PCHD brush on quartz substrates (measured in transmission mode). Of special interest in all of these spectra are the bands between 3018 and 2858 cm^{-1}, which correspond to $-CH_2-$ stretching modes; these can be used to qualitatively evaluate the extent of the aromatization (dehydrogenation) reaction. Although quartz substrates absorb IR radiation below 2300 cm^{-1}, it is possible to see that the bands present between 3018 and 2858 cm^{-1} for the PCHD brush completely disappear upon aromatization. Unfortunately the bands typically used to estimate the effective conjugation length of PPP (~805 cm^{-1}, corresponding to C−H out-of-plane bending of the 1,4-substituted phenyl rings, and ~760 and ~697 cm^{-1}, both corresponding to C−H out-of-plane vibration modes of monosubstituted phenyl rings)[14−16,50] are not accessible because of substrate absorption for both quartz and silicon wafers.

Figure 3 shows the UV-Vis spectrum of a PPP brush created by aromatization of an 11K PCHD brush. Similar results were obtained when the 4K and 19K PCHD brushes were aromatized, and those data can be found in the Supporting Information. There are clear differences between the UV-Vis spectra of PCHD precursor brushes (see inset in Figure 3) and the PPP brushes. After aromatization, two new absorption bands appear, the first being at 209 nm for each of the three molecular weights studied, and a second appears at 317, 320, and 323 nm for 4K, 11K, and 19K polymers, respectively. It is well-known that the position of this band depends on the effective conjugation length of the polymer,[12] and it has been used to estimate the effective conjugation length of PPPs by extrapolation of peak positions determined for oligo-paraphenylenes (OPPs).[7,11] However, most of these studies were made for OPPs in solution, and it can be misleading to infer thin film properties from these results. Therefore, we prepared a series of thin films made from OPPs, and their absorption characteristics are discussed next.

To compare and support the analysis of our results, we prepared thin films made of OPPs by spin coating and their UV-Vis absorption spectra are shown in Figure 6. As can be seen, two well-defined peaks are observed in each spectrum, with the position (of the maximum) of the second peak shifting to longer wavelengths as the number of phenyl rings increase. It is worth noting that the position of the maximum for the OPPs in thin films is red-shifted as compared to the values reported previously for these OPPs in dichloromethane.[11]

Table 2 lists the TD-DFT estimates of optical absorption for oligomers OPP-2 through OPP-7, first for the isolated chains, then for the systems grafted to the silica cluster. Overall, the theoretically predicted transition energies reproduce the trends observed by Banerjee et al.[11] for the isolated OPPs and mirror our results from measurements of OPP thin films. The absorption energies of the grafted system are red-shifted with respect to the isolated chain, with the magnitude of the shift decreasing with increasing oligomer size. We observe that the calculations overestimate the energy of the optical absorption band for the shorter oligomers, while underestimating the transition energies for $n \geq 3$, as compared to the experimental results on OPP thin films.

It has become customary to extrapolate results from OPPs to infer properties of high molecular weight PPPs. Usually a linear relationship between the energy associated with the second peak

dx.doi.org/10.1021/cm201819p |*Chem. Mater.* 2011, 23, 4367–4374

Table 2. TD-DFT B3LYP/LANL2DZ Electronic Absorptions of Oligomers OPP-2 through OPP-7 Grafted to a Silica Cluster Compared to the Isolated OPP Chains

		OPP-2	OPP-3	OPP-4	OPP-5	OPP-6	OPP-7
isolated oligomers	osc. strength	0.9	1.5	2.0	2.3	2.7	3.0
	energy (eV)	4.9	4.3	4.0	3.8	3.6	3.6
	wavelength (nm)	250	300	320	340	340	350
	exp. λ_{max} (nm)[a]	260	290	305	314	322	326
grafted to silica	osc. strength	0.9	1.4	1.7	2.0	2.4	2.7
	energy (eV)	4.7	4.1	3.9	3.7	3.6	3.5
	wavelength (nm)	260	300	320	340	340	350
	exp. λ_{max} (nm)[b]	260	290	310	320	330	

[a] As reported in ref 11 in dichloromethane solution. [b] OPP thin films spin-coated on silica, this work.

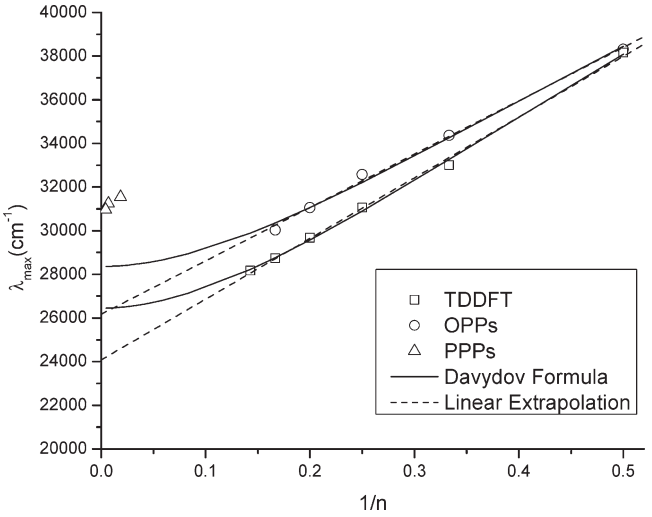

Figure 7. Position of second peak in the UV-Vis absorption spectra of OPP as a function of $1/n$. Open circles: experimental values for OPPs spin-coated on quartz. Open squares: TDDFT estimates for OPPs grafted to Silica. Two fits are shown; one is linear and the other uses the equation derived by Davydov.[12] Also shown are the peak positions measured for the three PPPs.

maximum and the inverse of the number of phenyl rings, n^{-1}, is used, with the optical properties for infinite molecular weight polymer inferred by extrapolation of this linear relationship.[7,11] The data are plotted in this fashion in Figure 7. However, it has been shown that the linear extrapolation, especially when based on short oligomers, fails to properly account for the saturation of the optical absorption energy with increasing conjugation length.[51−53]

An alternative analysis of the optical absorbance energy can be done using the equation derived by Davydov[12]

$$\Delta E_{min} = A - 2|M|\left|\mathrm{COS}\left[\frac{\pi}{(n+1)}\right]\right| \quad (1)$$

Here, ΔE_{min} is the transition energy of the corresponding conjugation band, n is the number of phenyl rings in the molecule, and the values of A and M are estimated to be 48 530 cm^{-1} and 10 086 cm^{-1}, respectively, from the experimentally determined peak position of the OPP films on quartz substrates used in this work (the same fit based on the TDDFT estimates results in A = 49 724 cm^{-1} and M = 11 636 cm^{-1}, see Figure 7). Figure 7 shows two lines that can be used to extrapolate to high n: one is a linear fit created from the data obtained for the series of OPPs on quartz substrates; the other line is obtained by fitting the equation derived by Davydov.[12] The former predicts that the peak position of an infinite molecular weight PPP polymer will be 364 nm, while the latter yields a value of 356 nm for an infinite MW PPP and also shows that the relationship between λ_{max} and $1/n$ is nonlinear, approaching the value for an infinite molecular weight PPP asymptotically. Even though the linear correlation developed from the OPPs agrees with predictions from TD-DFT calculations for surface deposited OPPs, it is evident that the simple linear fit grossly overestimates the adsorption band maximum for an infinite molecular weight PPP, regardless of whether it is grafted or surface adsorbed. Experimental observations using larger molecular weight oligomers have also confirmed this trend.[18] On the basis of the fit obtained using Davydov's equation and experimental data on OPPs, we estimate λ_{max} values of 355.5, 355.9, and 355.9 nm for the PPPs having n = 54, 146, and 238, respectively. However, as seen in Figure 7, we measure λ_{max} ~320 nm for all three cases, which corresponds to an effective conjugation length of ~5 units. A similar result is obtained by comparing the λ_{max} values measured with the values obtained by TD-DFT calculations shown in Table 2: an absorption wavelength of ~320 nm for the PPP brushes on quartz corresponds to an effective conjugation length of ~4 paraphenylene units. This should be considered a lower limit to the conjugation length, as the B3LYP/LANL2DZ results for the isolated oligomers suggest the calculations underestimate the absorption energy (overestimate the wavelength) for $n \geq 3$.

Comparison of the UV-Vis spectra of the OPPs (Figure 6) to that of the 11K PPP (Figure 3), shows that the shape of the spectra for the PPP is different than that of the OPPs; the PPPs show broader and less defined peaks. The first explanation to consider is that, as opposed to the OPPs, the PCHD precursor polymers are not exclusively made by 1,4 addition. The polar DABCO additive used during polymerization results in a chain microstructure that is 90−95% 1,4 addition (with the balance 1, 2 addition). These "defects" in microstructure along the chain would be present after aromatization and, therefore, reduce the effective conjugation length of the PPPs. Also, although our spectroscopy measurements indicate that aromatization was complete, it is possible that some of the repeat units (below the limits of detection) remain incompletely aromatized. In either case, these defects will be distributed along the brush chains, creating a distribution of conjugation lengths that could give rise to the broader shape of the absorption bands and peak positions observed in the UV-Vis spectra. Mulazzi et al. showed

that the experimentally observed shape of the UV-Vis spectrum of an electro-polymerized PPP could only be accounted for if a distribution of conjugated segments were included in the calculations.[54] The shape of the spectrum for their electro-polymerized PPP is similar to our results; however, the origin of the conjugation length distribution in each case is different: In the electro-polymerized PPPs, the chains are highly polydisperse and the chain microstructure content of 1,4 versus 1,2 linkages between repeat units is unknown. In our case, the polymers have very low polydispersities and high 1,4 content, which leads to the conclusion that the origin of the shape of the optical absorbance spectrum results from the distribution of conjugation lengths because of the chain microstructure. This hypothesis is supported by the results of Natori et al., who compared the optical properties of PPPs having nearly 100% and 50% 1,4 addition. They found that as the proportion of 1,2 addition increased, the peak present around 350 nm disappears completely for a chain having a 1:1 ratio of 1,4/1,2 content.[31] So even though the degrees of polymerization of our chains are considerably larger than 5 units, the presence of defects along the chain causes the spectra to change considerably.

SUMMARY AND CONCLUSIONS

End-functionalized PCHD polymers have been tethered to quartz and silicon surfaces and successfully aromatized in situ to create PPP brushes. Comparison of their UV-Vis spectra to that of thin films made by OPP supports the conclusion that the PPP chains consist of a distribution of 1,4 conjugated segments of different lengths. This distribution, which arises because of 1,2 linkages (defects) distributed along the chain length, gives rise to broader peaks in the UV-Vis absorption spectra as compared to the well-defined peaks for OPPs. For the high molecular weight PPP brushes made by in situ aromatization, the peak position of ~320 nm corresponds to an effective conjugation length of ~5 units. The grafting density of the chains on the surface can be manipulated by controlling the deposition conditions, and the influence of this parameter on the properties of high molecular weight-aromatized brushes can now be studied. The brushes before and after aromatization show complete surface coverage, with an increase in surface roughness occurring after aromatization, however the film quality remains very good, with no significant number of defects (pinholes or large aggregates). The approach used overcomes solubility issues associated with high molecular weight PPPs, allowing PPP to be processed in thin film form, engendering opportunities to create devices such as organic photovoltaic cells, vapor sensors, or field-effect transistors based on well-defined π-conjugated polymers as active layers.

ASSOCIATED CONTENT

Supporting Information. Measured thicknesses and calculated grafting densities, additional UV-Vis spectra, structural models used for the DFT calculations, computed TDDFT transition energies and oscillator strengths for all electron basis versus the LANL2DZ effective core potential, and correlation between ellipsometric and UV-Vis measurements used to estimate PCHD thicknesses on quartz substrates. This material is available free of charge via the Internet at http://pubs.acs.org.

AUTHOR INFORMATION

Corresponding Author

*E-mail: kilbeysmii@ornl.gov (M.K.).

ACKNOWLEDGMENT

This research was conducted at the Center for Nanophase Materials Sciences, which is sponsored at the Oak Ridge National Laboratory by the Office of Science, Department of Energy. This work was supported in part through the DOE Laboratory Directed Research and Development award program (awards 5090 and 5388). We thank Professor Rajendra Rathore from Marquette University for generously providing the OPPs used in this study.

REFERENCES

(1) Wallace, G. G.; Dastoor, P. C.; Officer, D. L.; Too, C. O. *Chem. Innov.* **2000**, *30* (4), 15–22.
(2) Zotti, G.; Vercelli, B.; Berlin, A. *Acc. Chem. Res.* **2008**, *41* (9), 1098–1109.
(3) Kanicki, T. J. In *Handbook of Conducting Polymers*, Skotheim, T. A., Ed.; Dekker: New York, 1986; pp 543−660.
(4) Yang, X.; Loos, J. *Macromolecules* **2007**, *40* (5), 1353–1362.
(5) Hopper, H.; Sariciftci, N. S. *J. Mater. Chem.* **2006**, *16*, 45–61.
(6) Radbeh, R.; Parbaile, E.; Boucle, J.; Di Bin, C.; Moliton, A.; Coudert, V.; Rossignol, F.; Ratier, B. *Nanotechnology* **2010**, *21* (3).
(7) Niko, A.; Meghdadi, F.; AmbroschDraxl, C.; Vogl, P.; Leising, G. *Synth. Met.* **1996**, *76*, 177–179.
(8) Wise, D. L.; Wnek, G. E.; Trantolo, D. J.; Cooper, T. M.; Gresser, J. D., *Photonic Polymer Systems: Fundamentals, Methods, And Applications*; Marcel Dekker: New York, 1998.
(9) Berresheim, A. J.; Muller, M.; Mullen, K. *Chem. Rev.* **1999**, *99* (7), 1747–1785.
(10) Shacklette, L. W.; Chance, R. R.; Ivory, D. M.; Miller, G. G.; Baughman, R. H. *Synth. Met.* **1980**, *1* (3), 307–320.
(11) Banerjee, M.; Shukla, R.; Rathore, R. *J. Am. Chem. Soc.* **2009**, *131* (5), 1780–1786.
(12) Suzuki, H. *Bull. Chem. Soc. Jpn.* **1960**, *33* (1), 109–114.
(13) Seoul, C.; Song, W. J.; Kang, G. W.; Lee, C. H. *Synth. Met.* **2002**, *130* (1), 9–16.
(14) Gin, D. L.; Avlyanov, J. K.; MacDiarmid, A. G. *Synth. Met.* **1994**, *66* (2), 169–175.
(15) Song, W. J.; Seoul, C.; Kang, G. W.; Lee, C. *Synth. Met.* **2000**, *114*, 355–359.
(16) Li, C.; Shi, G. Q.; Liang, Y. Q. *Synth. Met.* **1999**, *104* (2), 113–117.
(17) Miyashita, K.; Kaneko, M. *Synth. Met.* **1995**, *68* (2), 161–165.
(18) Remmers, M.; Muller, B.; Martin, K.; Rader, H.-J. *Macromolecules* **1999**, *32*, 1073–1079.
(19) Milner, S. T. *Science* **1991**, *251*, 905–914.
(20) Milner, S. T.; Witten, T. A.; Cates, M. E. *Macromolecules* **1988**, *21*, 2610–2619.
(21) Milner, S. T.; Witten, T. A.; Cates, M. E. *Europhys. Lett.* **1988**, *5* (5), 413–418.
(22) Toomey, R.; Mays, J. W.; Tirrell, M. *Macromolecules* **2004**, *37*, 905–911.
(23) Tian, P.; Uhrig, D.; Mays, J. W.; Watanabe, H.; Kilbey, S. M., II *Macromolecules* **2005**, *38*, 2524–2529.
(24) Alonzo, J.; Huang, Z.; Liu, M.; Mays, J.; Toomey, R.; Dadmun, M. D.; Kilbey, S. M., II *Macromolecules* **2006**, *39* (24), 8434–8439.
(25) Huang, Z.; Alonzo, J.; Liu, M.; Ji, H.; Yin, F.; Smith, G. S.; Mays, J. W.; Kilbey, S. M., II; Dadmun, M. D. *Macromolecules* **2008**, *41* (5), 1745–1752.
(26) Alonzo, J.; Mays, J.; Kilbey, S. M., II *Soft Matter* **2009**, *5* (9), 1897–1904.
(27) Kilbey, S. M., II; Watanabe, H.; Tirrell, M. *Macromolecules* **2001**, *34*, 5249–5259.
(28) Ayres, N. *Polym. Chem.* **2010**, *1* (6), 769–777.
(29) Uhrig, D.; Mays, J. W. *J. Polym. Sci., Part A: Polym. Chem.* **2005**, *43* (24), 6179–6222.
(30) Hong, K. L.; Mays, J. W. *Macromolecules* **2001**, *34* (4), 782–786.

(31) Natori, I.; Natori, S.; Sekikawa, H.; Sato, H. *J. Polym. Sci., Part A: Polym. Chem.* **2008**, *46* (15), 5223–5231.
(32) Natori, I.; Sato, H. *Polym. Int.* **2007**, *56* (6), 810–815.
(33) Natori, I.; Sato, H. *J. Polym. Sci., Part A: Polym. Chem.* **2006**, *44* (2), 837–845.
(34) Becke, A. D. *J. Chem. Phys.* **1993**, *98* (7), 5648–5652.
(35) Stephens, P. J.; Devlin, F. J.; Chabalowski, C. F.; Frisch, M. J. *J. Phys. Chem.* **1994**, *98* (45), 11623–11627.
(36) Jamorski, C.; Casida, M. E.; Salahub, D. R. *J. Chem. Phys.* **1996**, *104* (13), 5134–5147.
(37) Bauernschmitt, R.; Ahlrichs, R. *Chem. Phys. Lett.* **1996**, *256* (4−5), 454–464.
(38) Bauernschmitt, R.; Haser, M.; Treutler, O.; Ahlrichs, R. *Chem. Phys. Lett.* **1997**, *264* (6), 573–578.
(39) Hirata, S.; Head-Gordon, M. *Chem. Phys. Lett.* **1999**, *314* (3−4), 291–299.
(40) Valiev, M.; Bylaska, E. J.; Govind, N.; Kowalski, K.; Straatsma, T. P.; Van Dam, H. J. J.; Wang, D.; Nieplocha, J.; Apra, E.; Windus, T. L.; de Jong, W. *Comput. Phys. Commun.* **2010**, *181* (9), 1477–1489.
(41) Hay, P. J.; Wadt, W. R. *J. Chem. Phys.* **1985**, *82* (1), 270–283.
(42) Wadt, W. R.; Hay, P. J. *J. Chem. Phys.* **1985**, *82* (1), 284–298.
(43) Hay, P. J.; Wadt, W. R. *J. Chem. Phys.* **1985**, *82* (1), 299–310.
(44) Krishnan, R.; Binkley, J. S.; Seeger, R.; Pople, J. A. *J. Chem. Phys.* **1980**, *72* (1), 650–654.
(45) Jacquemin, D.; Wathelet, V.; Perpte, E. A.; Adamo, C. *J. Chem. Theory Comput.* **2009**, *5* (9), 2420–2435.
(46) Goerigk, L.; Moellmann, J.; Grimme, S. *Phys. Chem. Chem. Phys.* **2009**, *11* (22), 4611–4620.
(47) DiStefano, T. H.; Eastman, D. E. *Solid State Commun.* **1971**, *9* (24), 2259–2261.
(48) Tran, Y.; Auroy, P. *J. Am. Chem. Soc.* **2001**, *123* (16), 3644–3654.
(49) Yun, S. I.; Terao, K.; Hong, K.; Melnichenko, Y. B.; Wignall, G. B.; Britt, P. F.; Mays, J. W. *Macromolecules* **2006**, *39* (2), 897–899.
(50) Castiglioni, C.; Gussoni, M.; Navarrete, J. T. L.; Zerbi, G. *Mikrochim. Acta* **1988**, *1* (1−6), 247–249.
(51) Zade, S. S.; Bendikov, M. *Org. Lett.* **2006**, *8* (23), 5243–5246.
(52) Zade, S. S.; Zamoshchik, N.; Bendikov, M. *Acc. Chem. Res.* **2011**, *44* (1), 14–24.
(53) Gierschner, J.; Cornil, J.; Egelhaaf, H. J. *Adv. Mater.* **2007**, *19* (2), 173–191.
(54) Mulazzi, E.; Ripamonti, A.; Athouel, L.; Wery, J.; Lefrant, S. *Phys. Rev. B* **2002**, *65*, 08524.